# Ballistic transport through coupled T-shaped quantum wires

Yuh-Kae Lin, Kao-Chin Lin and Der-San Chuu Department of Electrophysics, National Chiao Tung University 1001 Ta H such Road, H sinchu, 30050 Taiwan

(today)

### Abstract

The ballistic conductance of a coupled T-shaped sem iconductor quantum wire (CTQW) are studied. Two types of CTQW are considered, one of which is a -shaped quantum wire (QW) which consists of two transverse wires on the same side of the main wire and the other a -clone quantum wire (CQW) which consists of two transverse wires on the opposite sides of the main wire. The mode matching method and Landauer-Buttiker theory are employed to study the energy dependence of the ballistic conductance. Most of transmission proles of QW and CQW are found to be distinguishable for large separation d between the two transverse arms. The transmission probability manifests oscillatory behavior when d is increased. When a potential is added to the connection region, it results in decoupling or coupling e ects between the two T-shaped wires according to whether it is positive or negative. When magnetic elds are applied to CTQW, the transmission proles are found to be a ected profoundly even if the electrons pass through

Corresponding author em ail address: dschuu@cc.nctu.edu.tw; Fax:886-3-5725230; Tel:886-3-5712121-56105.

the eld free region only.

71,23,An;7124.+q;7322.-f

Typeset using REVT<sub>E</sub>X

Recently, the microetching and epitaxial grow th techniques have enabled semiconductor nanostructures to be fabricated with feature sizes down to nanom eters. Such nanostructures include T-shaped quantum wires in which quasi-one-dimensional connement is achieved at the intersection of two quantum wells. Both experimental and theoretical studies on the nonlocal ballistic transport of these structures have been stimulated. In general, T-shaped quantum wires can be fabricated by rst growing a G aA s/A  $l_x$ G  $a_1$  \_xA smultilayers on a (001) substrate, after cleavage, a G aA s quantum well is grown over the exposed (110) surface, resulting in an anay of T-shaped quantum wires (TQW) possess some in proved optical properties of one dimensional excitons, such as the excitonic laser emission, the enhancement of excitonic binding energy, and the concentrated oscillator strength. The conductance of such a mesoscopic structure exhibits many peculiar and interesting features due to its intrinsic nonlocality. Quantum conductance in mesoscopic structures is the consequence of a complex scattering process which involves the boundary and the shape of the potential across the structural geometry as a whole.

Several studies on the electronic transm ission properties for a T-shaped quantum structure have been carried out.<sup>18</sup> M any interesting transm ission characteristics, such as resonant transm ission and resonant rejection in the T-shaped structures have been revealed. Such behaviors are caused from the quantum interference which dominates the ballistic transport regime. Theoretically, one may view the resonance as being mediated by the quasibound states of the system. The system of T-shaped quantum wires has open geometry, therefore, the injected carriers that travel ballistically over the wire region will across the wire region and show a strong energy dependent transm ission as a consequence of quantum interference e ect induced by the interplay between the propagating modes of the wires.

By using the scattering matrix approach and Landauer-Buttiker theory, Goldoniet. al.<sup>4</sup> have calculated the conductance of T-shape and coupled T-shaped quantum wires with dif-

ferent wire widths. The transmission coe cient of the whole coupled T-shaped quantum wires can be obtained easily since the total T-matrix is the product of the T-matrices of the isolated wires. The double resonance obtained in their result is ascribed to a ngerprint of the bonding and antibonding combinations of the resonance states of the isolated wires. Bohn<sup>5</sup> has introduced a periodic array of T-shaped devices. He showed that de ected arrays exhibit a unique resonance structure with respect to electrons traveling along the array. The coe cients of the relection and transmission through the array can peak simultaneously at resonance. Unlike the analogous case in superlattices, the peaks are at energies where the wavelength satisfies the condition n = 2 = d for some integer n. Consequently, the scattering wave function possesses nodes at the intersection of the longitudinal arm and the transversal arm, and thus greatly reduces the ux lost to transversal leads. Nikolic and Sordan<sup>67</sup> have also studied the transmission properties of a quantum waveguide system with attached stubs in the ballistic regime. They found the transconductance and the di erential drain conductance are small. Their result suggests limited abilities for conventional application of the transistor. Chen et. al.<sup>7</sup>. calculated transmission of electrons in a T-shaped opened quantum waveguide (TOQW) subjected to an inhom ogeneous magnetic eld perpendicular to the TOQW plane with mode-matching technique. The transmission pro les are found to depend sensitively on geometric parameters.

In this work, we study a -shaped opened quantum structure and its clone shape, which are four-term inal waveguide-like structures, schem atically as shown in Fig.1. We take rst the geometric variation into account. Second, the interconnection region is considered to be acted by a potential. Third, the magnetic eld is considered to apply to the vertical wires. Unlike the stubs, arm s of the structures considered in our case are assumed to be long enough and open in the longitudinal and the transverse directions. The centers of the two vertical arm s are spaced by a distance d as shown in Fig.1. The scattering matrice are calculated by using mode-mathing method. Our model will be presented brie y in the next section. Results and discussions will be given in the nal section.

W e model the structure geometry as illustrated in Fig.1: A horizontal wire with a width of W<sub>1</sub> (W<sub>2</sub>) for region I (V II), a vertical wire with a width of W<sub>2</sub> (W<sub>3</sub>) for region II (V), an interconnection part for region IV and a junction region with an area of W<sub>1</sub> W<sub>2</sub> (W<sub>1</sub> W<sub>3</sub>) for region III (V I). In the wire, 2D EG system with perfect barrier con nem ent (e.g. high quality interfaces) is assumed. The individual electron propagates ballistically through the entire wire. The transverse potential inside the wire is set to zero. The Schrödinger equation of individual electron can be written as

$$\frac{h^2}{2m}r^2 = E \tag{1}$$

The whole quantum wire can be split into x weral individual hom ogeneous subregions: horizontal region I, vertical regions II and V, intersection region III and VI, interconnecting region IV, and the outgoing horizontal region VII. The two intersection regions act as scattering centers. And the interconnecting region acts as a connection of the two TQW s. An nth mode electron is considered to inject from left of region I into the wire. The wave function in region I can be written in terms of a sum of incident and re ecting modes as

$$\prod_{n}^{I} (x; y) = \prod_{n}^{I(+)} (y) e^{ik_{n}^{I(+)} (x+0.5W_{2})} + \prod_{m}^{X} R_{mn} \prod_{m}^{I(-)} (y) e^{ik_{m}^{I(-)} (x+0.5W_{2})};$$
(2)

where  $k_n^{I()} = \frac{q}{k^2} (n = W_1)^2$ ; represents the incident or rejecting mode, respectively, and  $\prod_{n=1}^{I()}$  are envelope functions in region I. The wave functions in regions II, V, and V II are given by a sum of outgoing modes respectively, i.e.,

$$\prod_{n}^{II} (x; y) = \int_{m}^{X} S_{mn}^{(1)} \prod_{n}^{II(+)} (x) e^{ik_{m}^{II(+)} (y \ 0.5W_{1})};$$
(3)

$$S_{m}^{(2)}(\mathbf{x};\mathbf{y}) = \int_{m}^{X} S_{mn}^{(2)}(\mathbf{x}) e^{ik_{m}^{(1)}(\mathbf{y})(\mathbf{x})} e^{ik_{m}^{(1)}(\mathbf{y})(\mathbf{x})}$$
(4)

where represents the upward or downward arm and

$$\sum_{n}^{V \text{ II}} (x^{0}; y) = \sum_{m}^{X} T_{m n} \sum_{m}^{V \text{ II} (+)} (y) e^{ik_{m}^{V \text{ II} (+)} (x^{0} 0 : 5W_{3})}$$
(5)

The wave function in region IV is given by the sum of rightgoing (+) and leftgoing () modes,

$$\sum_{n}^{IV} (x; y) = \sum_{m}^{V} U_{m n} \sum_{m}^{IV (+)} (y) e^{ik_{m}^{IV (+)} (x - 0.5W_{2})} + V_{m n} \sum_{m}^{IV (-)} (y) e^{ik_{m}^{IV (-)} (x - 0.5W_{2})} :$$
(6)

In region III and region V I, all modes must be taken into account, thus

$$\prod_{n}^{III} (\mathbf{x}; \mathbf{y}) = \begin{cases} X & h & i \\ f_{j}(\mathbf{y}) & a_{jn} \sin k_{j}^{0}(\mathbf{x} & 0.5W_{2}) + b_{jn} \sin k_{j}^{0}(\mathbf{x} + 0.5W_{2}) \\ & + & g_{j}(\mathbf{x}) c_{jn} \sin k_{j}^{00}(\mathbf{y} + 0.5W_{1}) ; \end{cases}$$
(7)

$$\sum_{n}^{VI} (x^{0}; y) = \sum_{j=1}^{X} f_{j}(y) d_{jn} \sin k_{j}^{0} (x^{0} - 0.5W_{3}) + e_{jn} \sin k_{j}^{0} (x^{0} + 0.5W_{3}) + g_{j}^{0} (x^{0}) h_{jn} \sin k_{j}^{00} (y - 0.5W_{1}) + g_{j}^{0} (x^{0}) h_{jn} \sin k_{j}^{00} (y - 0.5W_{1})$$
(8)

Here  $f_j(y) = {q \over {2 \over W_1}} \sin {j \over W_1} (y + 0.5W_1)$ ;  $g_j(x) = {q \over {2 \over W_2}} \sin {j \over W_2} (x + 0.5W_2)$  and  $g_j^0(x^0) = {q \over {2 \over W_3}} \sin {j \over W_3} (x^0 + 0.5W_3)$  represent the transverse wave functions of the electron in mode j inside the di erent regions of the wires, and are used as the expansion bases. The wave numbers  $k_j^0 = {q \over K^2} (j = W_1)^2$ ;  $k_j^0 = {q \over K^2} (j = W_2)^2$ ; and  $k_j^0 = {q \over K^2} (j = W_3)^2$  are either real for propagating modes or pure in aginary for evanescent modes. Now expand the wave-functions in terms of a set of complete bases corresponding to the transverse eigenfunctions in regions I, II, IV, V and V II, respectively as

$$\int_{n}^{I()} (y) = \int_{jn}^{X} f_{j}(y);$$
(9)

$$\prod_{n}^{\text{II}(+)}(\mathbf{x}) = \prod_{j=1}^{X} \prod_{j=1}^{\text{II}(+)} g_{j}(\mathbf{x});$$
(10)

$$\prod_{m}^{IV()}(y) = \prod_{jm}^{X} \prod_{jm}^{IV()} f_{j}(y);$$
(11)

$$\sum_{n}^{v(i)} (x^{0}) = \sum_{jn}^{X} \sum_{jn}^{v(i)} g_{j}^{0} (x^{0});$$
(12)

and

$$\sum_{n}^{V II(+)} (y) = \sum_{jn}^{V II(+)} f_{j}(y):$$
(13)

Substituting these functions into Eq.(1) for a given Ferm i energy  $E_F$ , we obtain ve sets of eigen-wave-numbers  $fk_n^{I()}g$ ,  $fk_n^{II(+)}g$ ,  $fk_n^{IV()}g$ ,  $fk_n^{V()}g$ , and  $fk_n^{VII(+)}g$  and eigen-wave-functions  $f_n^{I()}(y)g$ ,  $f_n^{II(+)}(y)g$ ,  $f_n^{IV()}(y)g$ ,  $f_n^{V()}(y)g$ , and  $f_n^{VII(+)}(x)g$ . By using boundary matching technique,<sup>9</sup> we can derive all coe cients in Eqs. (2) { (8) such as  $fr_{mn}g$ ,  $fs_{mn}^{(1)}g$ ,  $fs_{mn}^{(2)}g$ ,  $fu_{mn}g$ ,  $ft_{mn}g$ ,

The group velocities of the j th state in region I, II, V and VII are respectively

$$V_{j}^{I()} = \frac{h}{m} \frac{\sum_{0:5W_{1}} I()}{\sum_{0:5W_{1}} j} (y) k_{j}^{I()} I() (y) dy;$$
(14)

$$V_{j}^{II(+)} = \frac{h}{m} \int_{0.5W_{2}}^{Z_{0.5W_{2}}} \int_{j}^{II(+)} (x) k_{j}^{II(+)} \int_{j}^{II(+)} (x) dx; \qquad (15)$$

$$V_{j}^{V(\cdot)} = \frac{h}{m} \int_{0:5W_{3}}^{2} \int_{0:5W_{3}}^{0:5W_{3}} \int_{j}^{V(\cdot)} (x) k_{j}^{V(\cdot)} \int_{j}^{V(\cdot)} (x) dx;$$
(16)

aswellas

$$V_{j}^{VII(+)} = \frac{h}{m} \int_{0.5W_{1}}^{Z_{0.5W_{1}}} \int_{j}^{VII(+)} \langle y \rangle k_{j}^{VII(+)} \int_{j}^{VII(+)} \langle y \rangle dy:$$
(17)

The transmission probabilities  $\mathfrak{E}_{nj}$  (in region VII) and  $\mathbf{s}_{nj}^{(1)}$   $\mathbf{s}_{nj}^{(2)}$  (in region II and region V) from the incident moden to the nalmode j, and the rejection probability  $\mathbf{E}_{nj}$  from the incident moden to the nalmode j (in region I) can be obtained, respectively, as follows:

$$\mathbf{E}_{nj} = \frac{V_{j}^{I(+)}}{V_{n}^{I(+)}} jr_{nj} j^{2};$$
(18)

$$\mathbf{s}_{nj}^{(1)} = \frac{V_{j}^{III(+)}}{V_{n}^{I(+)}} j s_{nj}^{(1)} j^{2};$$
(19)

$$\mathbf{s}_{nj}^{(2)} = \frac{V_{j}^{III(+)}}{V_{n}^{I(+)}} j s_{nj}^{(2)} j;$$
(20)

$$\mathbf{e}_{nj} = \frac{V_{j}^{II(+)}}{V_{n}^{I(+)}} jt_{nj} j^{2} :$$
 (21)

It should be emphasized that the expansions (9) { (13) involve an in nite sum including all possible evanescent modes. In practice, in order to solve this set of equations numerically, we have to truncate the sum at some nite number which should be large enough to achieve a desired accuracy. The numerical convergence can be checked by ux conservation. The relationship  $P_{j}$  ( $\mathfrak{E}_{jn} + \mathfrak{E}_{jn} + \mathfrak{s}_{jn}$ ) = 1 should be fulled accurately.

The total transmission coe cients T and S are then given by

$$\mathbf{T} = \sum_{\substack{n=1 \ j=1}}^{\aleph_1} \Re_2 \mathbf{e}_{nj}; \tag{22}$$

$$S = \sum_{\substack{n=1 \ j=1}}^{N_1} \mathbf{s}_{n\,j} :$$
(23)

W here  $N_1$ ,  $N_2$  and  $N_3$  are the numbers of propagating modes in regions I, II and III, respectively. The conductance G at zero temperature is given by the Landauer{Buttiker formula:

$$G_t = (2e^2 = h)T$$
 (24)

and

$$G_s = (2e^2 = h)S:$$
 (25)

We also evaluate the probability density of electrons in the quantum wire by adding the contributions from all propagating modes as

$$(x;y) = \sum_{n=1}^{X^{N}} j_{n}(x;y) j^{2} = k_{n}:$$
 (26)

### III.NUMERICAL RESULTS AND DISCUSSIONS

#### A. Transm ission Properties with Geometric Variations

Figs.1 (a) and (b) schem atically depict the geometry of the  $\{\text{shaped } QW \ (QW)\}$  and the  $-\text{clone } QW \ (CQW)$ . We present our results in terms of some convenient parameters:

1) the nst threshold energy  $E_1 = \frac{h^2}{2m} (=W_1)^2$  through horizontal wire, 2) the distance d between two center of the intersections of vertical wires and horizontal wire, 3) the ratios of widths  $= W_2 = W_1$  and  $= W_3 = W_2$ .

First of all, we consider that all wires are the same width, namely W. Transmission probabilities are calculated with varying  $k_F$  as shown in Fig. 2(a) and (b) for di erent d. Curves from bottom to top in Fig.2(a) are shifted by 1.0 for clarity and correspond to the cases of d = 1, 1.1, 1.2, 1.3, 1.5, 1.7, and 2.0W<sub>1</sub>, respectively. And curves from bottom to top in Fig.2(b) are shifted by 1.0 for clarity and correspond to the cases of d = 2, 2.5, 3.0, and 5.0W<sub>1</sub>, respectively. Hereafter, we present the transmission probabilities of the QW system as solid lines and those of the CQW system as the dotted lines in all gures.

For d = 1, the vertical wires are adjacent to each other. Thus, a QW with d = 1, can be regarded as a TQW with a double width in the vertical arm except there is an in nite thin wall along the vertical arm axis. However, one can note from the gure that the proles of transmission of a QW with d = 1 are quite dierent from the transmission pro les of a TQW with the same width  $(2.0W_1)$  of the vertical arm<sup>8</sup>. In fact, the bottom curve of QW (d = 1) is similar to the result obtained in TQW with a vertical arm of  $1.0W_1$  width as obtained in Ref (8). This implies that the two systems are similar except the transmission amplitude is suppressed in a QW system. For the CQW, the sharp dip at  $k_F = 2.0 = W_1$  is replaced by a wider valley before  $k_F = 2.0 = W_1$ . The transmission behaviors of the two structures ( QW and CQW ) are dierent in general, however, their periodic oscillations are the same. The period of the oscillation is dom inated by the distance d as can be seen from Fig 2. The periodicity can be tted as  $n_1 = 2d$  approximately, where n is the number of periods in one mode, and  $1 = 2 = (k_F = W_1)$  denotes the longitudinal wave length of the incident electron waves. Thus, once one nds two peaks in the region  $1.0 < k_F W_1 = < 2.0$  for d = 1W<sub>1</sub>, then four peaks will be found for d = 2W<sub>1</sub>, and so on. Curves in both structures ( QW and CQW ) possess peak-dip structures. Especially, these peak-dip structures are more clear for larger d at  $k_F = 2.0 = W_1$ . On the contrary,

they are observed only in certain circum stance for smaller d. According to the previous result<sup>8</sup>, there exists a localized state in the intersection region for a symmetric TOQW with same wavenum ber  $k_F = 2.0 = W_1$ . The peak-dip structure at  $k_F = 2.0 = W_1$  can be ascribed to this localized state. The peak-dip structure is found at  $k_F = 2.0 = W_1$  on the curve with d = 1.5 for CQW. For d larger than  $1.5W_1$ , the peak-dip structure is sharper in CQW than that in QW.

Due to the fact that both QW and CQW structures are equivalent to a system of two TQW s, one may expect that the transmission properties of these two structures will be the same if the coupling between the constituent TQW s becomes very weak. However, our result does not manifest this accordance. On the contrary, the two transmission proles are still distinguishable from each other even for large d. It is also found that the transmission probabilities vary periodically with d for a xed wavenum ber as shown in Fig.3. These behaviors are the essential characteristics of ballistic theory.

Now let us consider the case that the widths of the vertical wires are the same, while the ratio of the width of the vertical wire to the horizontal wire is varied. The result is displayed in Fig. 4. For simplicity, we de ne the ratio of the width of the vertical wire to the horizontal wire as  $= W_2 = W_1 = W_3 = W_1$ . And the distance d is set to 2 W<sub>1</sub>. Curves from the bottom to the top are shifted by 1.0 individually for clarity and correspond to the cases of = 0.1, 0.2, 0.3, 0.5, 0.7, 1.0, 1.5, 2.0 and 4.0, respectively, as shown in the gure. For extrem ely sm all , perfect stepw ise pro les are observed in both structures. The transm issions are strongly suppressed when the ratio is large (e.g. 2.0 and 4.0). The solid curve for = 0.5 agrees with the result of previous work<sup>4</sup>. A double resonance is evident either on the curve of = 0.3 or the curve of = 0.5. They are the signature of the bonding and antibonding combinations of the resonant quasi-1D state of isolated wires.

Finally, the transmission proles in the QW and CQW with vertical wires of dierent width are considered. For simplicity, the width of one vertical wire is kept to be the same as that of the horizontal wire. The calculated transmission proles for  $W_1 = W_3$  and dierent  $W_2$  are shown in Fig.5(a) and those for  $W_1 = W_2$  and various  $W_3$  are shown in Fig.5(b).

Curves are o set for clarity. Curves from bottom to top correspond to the cases of = 0.1, 0.2, 0.3, 0.5, 0.7, 1.0, 2.0, 4.0, and 5.0, respectively. Where is the ratio of the wire width of the vertical wire to the horizontal wire. It is observed that the transmission probability is drastically suppressed for large as can be seen from the upper curves in (a) and (b). C om paring curves in (a) and (b), we observe that the transmission pro les are the same. When is small, the transmission pro les of the QW and CQW become indistinguishable and alm ost the same as that of TQW system. The double resonance can be observed again.

#### B. Transm ission Under an Additional Potential

We now consider the case that an additional scalar potential is applied to the interconnection region IV. The applied potential can be negative or positive for attracting or depleting electrons. The di erent coupling proles are interesting and may be important for practical usage of the mesoscopic devices.

Fig.6 presents the calculated transm ission proles for dimential strength  $V_4$  in unit of E<sub>1</sub>. Here we consider W<sub>3</sub> = W<sub>2</sub> = W<sub>1</sub>, and d = 2W<sub>1</sub>. Figs.6 (a) and (c) correspond to the positive potential for electrons. Figs.6 (b) and (d) correspond to negative potential. Curves are one set for clarity. As shown in Fig.6 (a), one can observe that the positive potential does not a lect the transmission very much when  $V_4 = E_1$ . >From Figs.6 (a) and (c), two features are shown: (1) the onset is shifted due to the depletion potential; (2) the positions of transmission dips are not changed. On the contrary, Figs.6 (b) and (d) show that the additional negative potential a lects the transmission much stronger than the positive one. Especially, the potential enhances the coupling between the two TOQW s as one can note from the fact that the resonant dip-peak-dip structure becomes broader and shallower when the potential is increased. M ore peaks are on the curves and the positions of dips are not changed. M ore peaks are on the curves and the positions of dips are not changed as the case of positive potential. M oreover, it can be observed that discrepancy between the two structures becomes prominent as the potential strength is increased. These results manifest that the negative potential increases the coupling strength between the two

#### C. Transm issions under the in uence of surrounding magnetic Fields

Finally, magnetic elds are considered to apply to the vertical wires only, therefore, the electrons pass through the main arm regions with no additional eld. We shall study the e ect of the surrounding magnetic elds on the transmission behavior. First, we consider the magnetic eld is applied only to one of the vertical wires, ie on am II or am V. The direction of the eld is perpendicular to the 2DEG plane. Transm ission probabilities are calculated as a function of Ferm i wave vector as depicted in Fig.7. Curves in Fig.7(a) are o set for clarity, and correspond to the cases of magnetic eld strength B = -1.0, -0.7, -0.5, -03, -02, -01, 01, 02, 03, 05, 0.7, 1.0 Tesla, respectively in region II. Those shown in Fig.7 (b) are the same except the magnetic eld is applied to region V.>From these curves, one can conclude that: (1) the magnetic eld does a ect the transmission, although the electrons do not pass through the region with magnetic eld directly. This phenom enon is according with A haronov-Bohm e ect. However, no periodic behavior can be found. (2) For the QW system as shown in solid curves in Figs.7 (a) and (b), both cases show a one-to-one correspondence to each other. This manifests that the in uence of the magnetic eld on the transm ission pro le depends only on the magnetic eld strength. However, there is no correspondence in the case of CQW which is presented by the dotted lines in Figs.7 (a) and (b). (3) Generally speaking, opposite polarity of the magnetic eld causes di erent in uence on the transmission in CQW systems.

The transm ission proles versus Ferm i wave number  $k_F$  for the case that the magnetic eld being applied to both regions II and V, are displayed in Fig.8. Fig.8(a) presents the transm ission in the QW s and CQW s with same polarity in both vertical arms, and Fig.8(b) presents those with opposite polarity to each other in the two vertical arms. The curves are o set for clarity. The solid lines represent the QW systems and dotted lines represent the CQW s systems. It is found that for the case of QW s, though the geometry

and the applied eld are symmetric, the transmission probabilities are dimension from each other (e.g. the solid curves with v = 0.2 and 0.2) as can be seen from Fig.8 (a). However, for the case of CQW s, the transmission are polarity independent as can be noted from the dotted curves in Fig.8 (a). No such symmetry can be found in CQW as shown in Fig.8 (b). Furthermore, peak-dip structures are evident both in Figs. (a) and (b) at high eld situations, though the electrons always move in eld free region. One can expect that the transmission pro les will become stepwise structures when the applied magnetic eld is extremely high. And in the intermediate eld strength, the magnetic eld changes the oscillatory behavior of the pro les signi cantly.

#### IV.SUMMARY

In the present work, the transm ission properties of the coupled TOQW s are found to be very sensitive to the geometric congurations as well as the strength and polarity of the applied elds. A double resonance is observed on the proles at certain ratio of the width of the vertical wire to the horizontal wire. The transm ission is suppressed drastically as the width of one or both vertical wires become large. Most of the transm ission proles of QW and CQW are distinguishable even for large inter-distance d between the two vertical wires. The transm ission proles exhibit oscillatory behavior as the distance d is increased and manifest periodic features as the distance d is varied. T-shaped quantum wires have been proposed to achieve the quantum interference e ect by controlling the length of its lateral closed arm s. In the present study, it is found that the interference pattern can be easier to obtain by modulating the length and width of transversal arm s and the distance between arm s.

W hen a potential is added to the connection region, it results in decoupling or coupling e ects between the two TQW s according to whether it is positive or negative. This behavior is observed by the alternating occurrence of the successive dips and valleys when the potential is increased positively.

Though the electrons pass through only the eld free region, the magnetic eld still a ects the transmission in the QW s profoundly. The perfect transmission can be seen only in the high magnetic eld region.

A know ledgem ent: This work is supported partially by N ational Science C ouncil, Taiwan under the grant num ber NSC 91-2112-M -009-002.

## REFERENCES

- [1] F. Sols, M. Macucci, U. Ravaili, and K. Hess, J. Appl. Phys. 66, 3892 (1989); F. Sols and M. Macucci, Phys. Rev. B 41, 11887 (1990).
- [2] JW ang and H G uo, ApplP hys. Lett. 60, 654 (1992).
- [3] R. Sordan and K. Nikolic, Appl. Phys. Lett. 68, 3599 (1996).
- [4] G. Goldoni, F. Rossi, and E. Molinari, Appl. Phys. Lett. 71, 1519 (1997).
- [5] J.L.Bohn, Phys. Rev. B 56,4132 (1997).
- [6] K. Nikolic and R. Sordan, Phys. Rev. B 58, 9631 (1998).
- [7] B. -Y. Gu, Y.K. Lin, and D.S. Chuu, J. Appl. Phys. 86, 1013 (1999); K.-Q. Chen, B.-Y. Gu, Y.K. Lin, and D.S. Chuu, Intl. J. Mod. Phys. B 13, 903 (1999)
- [8] Y K. Lin, Y N. Chen and D S. Chuu, Phys. Rev. B 64, 193316 (2001); J. Appl. Phys. 91, 3054 (2002).
- [9] J.Goldstone and R.L.Ja e, Phys. Rev. B 45, 14100 (1992).

#### FIGURES

FIG.1. (a) The schematic illustrations of the geometries of a QW system. (b) a CQW system.

FIG.2. The transmission T versus  $K_F$  for di erent dwhich is converted to v by d =  $(1 + v)W_1$ . All wires have same width. (a) d 2W<sub>1</sub> (b) d 2W<sub>1</sub>. The solid lines represent the T of QW, while the dotted lines represent the T of CQW.

FIG.3. The periodic behaviors of transm issions versus d for W<sub>3</sub> = W<sub>2</sub> = W<sub>1</sub>:  $T_1(T_2)$ ;  $S_1(S_2)$  represent the total transm ission coe cients T and S as de ned in Eqs.(22) and (23) for QW (CQW).

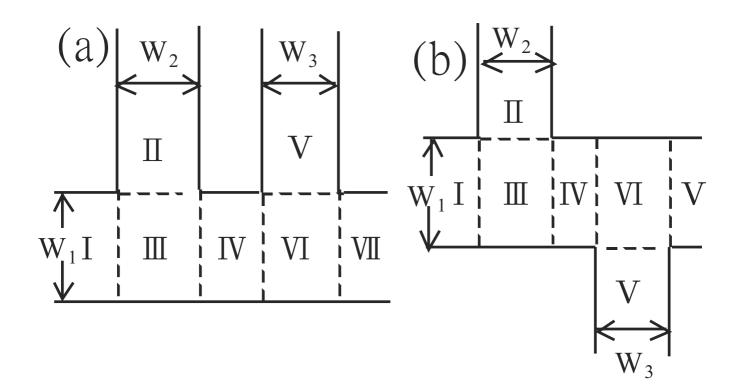
FIG.4. Transmission versus  $k_F$  for dierent . Where is the ratio of the width of the vertical arm to the horizontal arm . And d = 2 W<sub>1</sub>. The solid lines represent the T of QW, while the dotted lines represent the T of CQW. Curves are o set for clarity.

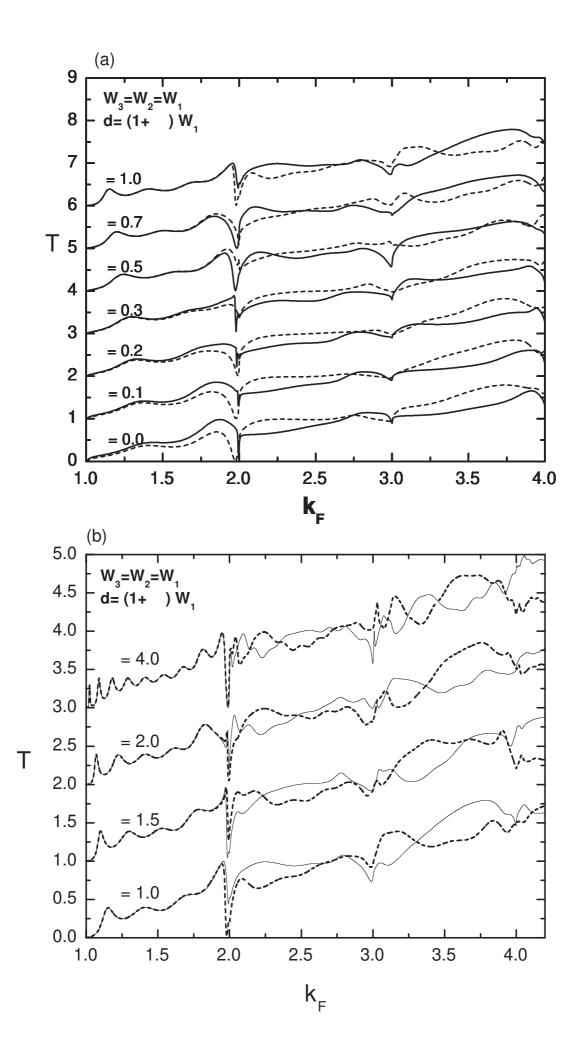
FIG.5. Same as Fig 2, except the width of one vertical arm varies. (a) The width of W  $_2$  varies, (b) the width of W  $_3$  varies. The solid lines represent the T of QW, while the dotted lines represent the T of CQW.

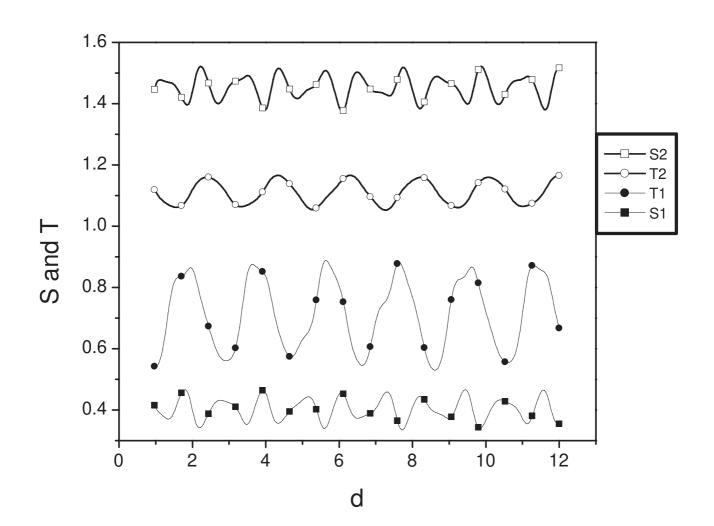
FIG.6. Transmission proles versus  $k_{\rm F}$  for a potential V<sub>4</sub> applied to the region IV. (a) and (c) correspond to the positive potential and (b) and (d) correspond to the negative potential. The solid lines represent the T of QW, while the dotted lines represent the T of CQW.

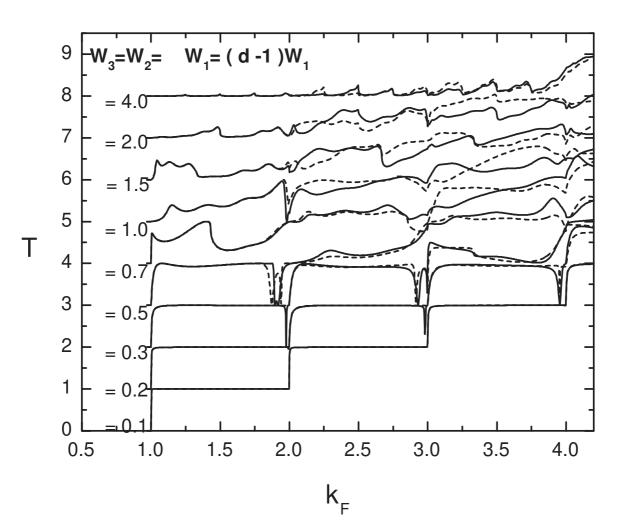
FIG.7. Transmission proles versus  $k_F$  for the magnetic eld applied to only one vertical arm. (a) to region II, and (b) to region V. The solid lines represent the T of QW, while the dotted lines represent the T of CQW. Curves are o set for clarity.

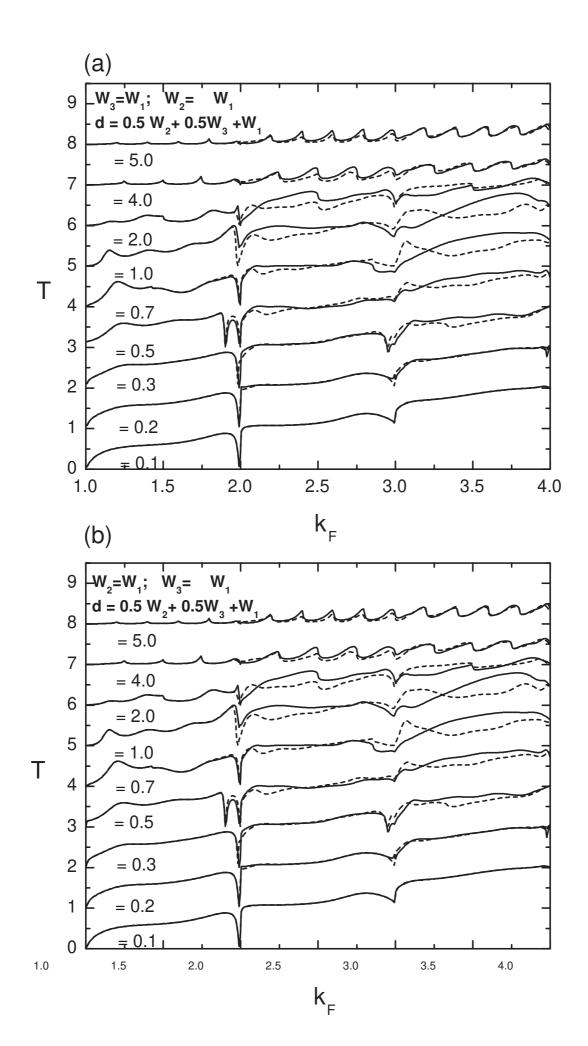
FIG.8. Transmission pro les versus  $k_{\rm F}$  for the magnetic eld applied to both vertical arms. (a) same polarity, and (b) opposite polarity in II and V. The solid lines represent the T of QW, while the dotted lines represent the T of CQW. Curves are o set for clarity.

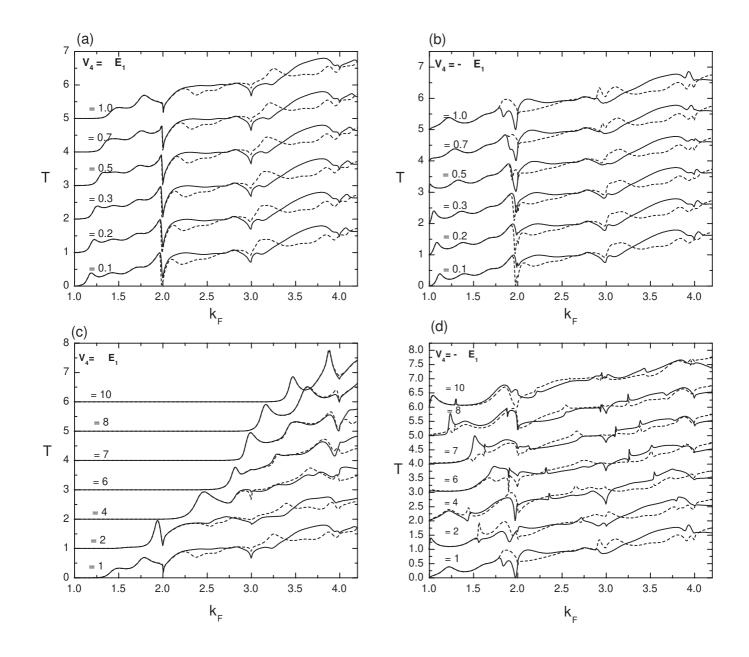


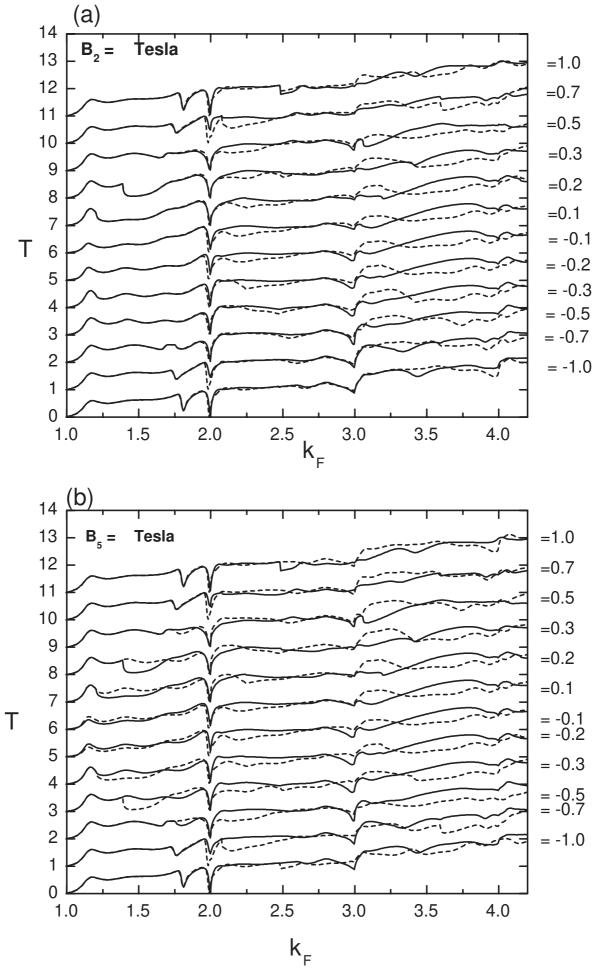


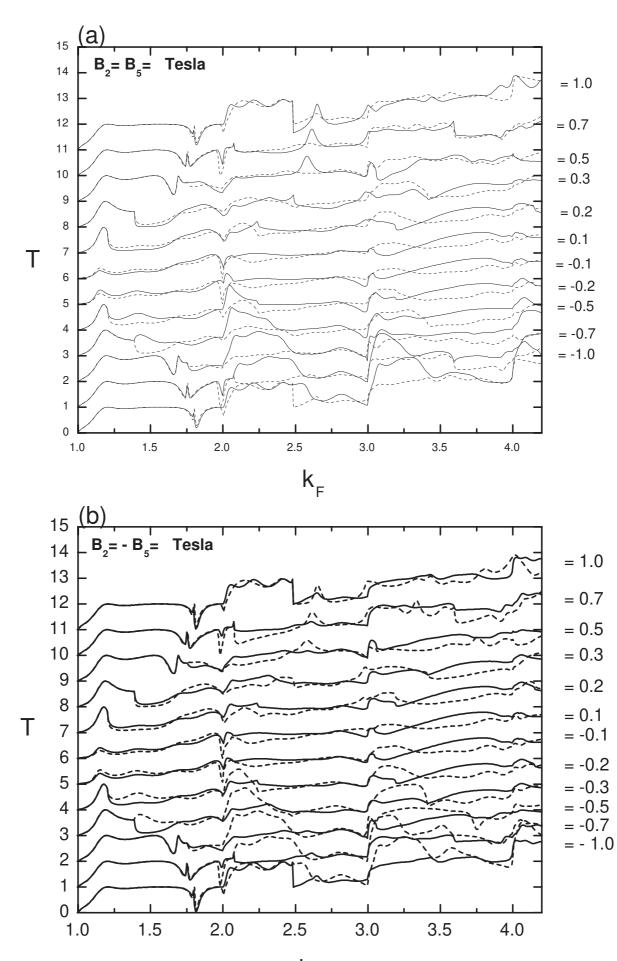












 $\mathbf{k}_{\mathrm{F}}$